PROCEEDINGS, Thirty-Eighth Workshop on Geothermal Reservoir Engineering
Stanford University, Stanford, California, February 11-13, 2013
SGP-TR-198

COLLAPSE ANALYSIS OF THE CASING IN HIGH TEMPERATURE GEOTHERMAL WELLS

Gunnar Skúlason Kaldal[1]*, Magnús Þ. Jónsson[1], Halldór Pálsson[1], Sigrún N. Karlsdóttir[1,2]

[1] Faculty of Industrial Engineering, Mechanical Engineering and Computer Science, University of Iceland, Hjarðarhagi 2-6, 107 Reykjavík, Iceland
[2] Innovation Center Iceland, Department of Materials, Biotechnology and Energy, Keldnaholt, Reykjavik, 112, Iceland
*e-mail: gunnarsk@hi.is

ABSTRACT

Casing failures such as collapse is the suspected result of combined loads and impurities in the casing and/or the surrounding concrete. In this paper a simple case of collapse caused by a geometric defect in the casing is analyzed using the finite-element method (FEM). The collapse of an impaired casing and its resulting shape is investigated with respect to the external supporting concrete. A specific load history for the production casing is used in the analysis. The first load consists of the external pressure of the cement slurry during well cementing, followed by subsequent cyclic thermal loads. The load history represents the fundamental loads which occur during the lifetime of a typical well. The magnitude of the external pressure and its stimulus for later collapse is also analyzed. The collapse shape obtained in the FEM analysis is similar to collapse shapes that have been observed in geothermal wells.

INTRODUCTION

High temperature geothermal wells are constructed of several concentric steel casings with cement in between the casing walls. The structural integrity of such well casings is essential for the utilization of high temperature geothermal wells. Casing failures can lead to a reduced energy output from the well, render the well inoperative and in worst cases cause unsafe conditions above the surface.

Casing failures such as collapse are the result of combined loads and impurities in the casing and/or surrounding concrete. Collapse or bulging of geothermal well casings is an example of a serious casing failure. Bulging is referred to as the buckling shape where the collapse occurs on one side of the cross section of the casing. This bulging collapse shape is related to the external support of the concrete and it only occurs when this support is present.

A well with a decreased cross sectional area, due to a collapsed production casing, produces less than an intact well, since the output of the well is proportional to the cross sectional area of the casing (Thorhallsson 2006). If the casing gets damaged, for example by tearing or collapse, the risk of well blow-out or more catastrophic well failures increases. Therefore, it's important to understand fully the structural system and its response to various loads during well operations. Accordingly, it is important to recognize the expected load history of the structure so that the deformation and stress fields that form during the lifetime of the well can be anticipated.

Analysis of the bulging collapse shape is the motivation for this paper. A simple case of collapse caused by a geometric defect in the casing is analyzed using the finite-element method (FEM). The collapse of the impaired casing and its collapse shape is investigated with respect to the presence of external supporting concrete.

The collapse of pipes in general has been profusely studied, often in connection to specific topics. Such analysis has been performed for the necessity of economical design and safety dating back to the end of the industrial revolution where the resistance of tubes to collapse was studied extensively and empirical equations were derived from numerous experiments (Fairbairn 1858). Since then many studies have been performed on the subject to improve empirical equations of pipe collapse. Casing collapse is highly dependant on geometrical imperfections of the casing. In collapse experiments, imperfections like the average outside diameter, average wall thickness, eccentricity and ovality have been measured and predicted with (empirical) equations (C. R. Kennedy et al. 1962, ISO/TR 10400:2007(E)). Collapse of well casings is an example of a specific case of pipe collapse. Collapse due to external pressure, e.g. during cementing, is similar to other cases of pipe collapse such as in deepwater sea-floor pipelines due to ambient external pressure. Effects of defects on the collapse pressure of pipes have been studied with experiments and finite element models (Assanelli et al. 1998,

Sakakibara et al. 2008, Netto 2009). The bulging collapse of well casings, that takes place during well operations after well completion, is a different case because of the lateral/radial support of the external concrete. This is to some extent comparable to horizontal soil supported pipes that have greater capacity to withstand net external pressures than pipes without support (Watkins and Anderson 2000). In well-compacted soil the cross section remains sensibly circular until failure by wall-buckling takes place (Bulson 1983). Likewise for burst design, the support of the external cement sheath increases the burst resistance of casings (Kalil et al. 2011). Collapse of pipes is caused by excessive net external pressure as well as instability due to various impurities. For concrete supported casings, instability in the casing to casing annulus is introduced, e.g. due to off centered casing and trapped fluid. Casing failure as a result of the expansion of trapped fluid in the annulus between casings has been discussed to a certain extent as a suspected cause of casing bulge collapse (Björnsson et al. 1978, Magneschi et al. 1995, Southon 2005).

In the remaining sections casing impurities and collapse loads are discussed, a three dimensional finite element model of a casing with a small geometrical defect is described, and finally collapse analysis results are presented and discussed.

CASING IMPURITIES AND COLLAPSE LOADS

A complete collapse of casings is a buckling shape that is governed by uniform external to internal differential pressure. The empirical equations used in standards for collapse resistance of casings is based on combined theoretical, numerical and statistical tools (ISO/TR 10400:2007(E)). These empirical equations do however not account for external supporting concrete and non-uniform loads and are also considered to be rather conservative.

In general, the ratio of outer diameter to thickness (D/t) determines whether collapse occurs in the elastic-, plastic- or intermediate range of the wall compressive stresses. For high values of the D/t ratio, elastic collapse is a governing factor. For lower values, the buckling occurs in the plastic range and for the lowest values the buckling is governed by the yield strength of the material (10400:2007(E) 2007). The critical elastic buckling pressure for long tubes under uniform radial pressure is

$$p_{cr} = \frac{E}{4(1-\nu^2)}\left(\frac{t}{R}\right)^3$$

(Timoshenko 1961, Bulson 1983, Chater and Hutchinson 1984) where ν is Poisson's ratio, E is Young's modulus, t is the tube thickness and R is the tube radius. This equation does however not account for collapse as a result of plastic deformation in the material which occurs in thicker casings. For thicker casings a tangent modulus, E_t is used in place of E, to find the critical buckling pressure beyond the proportional limit.

After completion of geothermal wells the concrete surrounding the production casing provides a structural support for the casing. When the well warms up, the concrete restrains the thermally expanding casing and limits both axial and radial movement to some extent. The bulging collapse shape, seen in Figure 1, only occurs in completed wells. The concrete support restricts the radial movement which results in a different collapse shape from that seen in casings without external support. Furthermore, the buckling shape suggests instability that is caused by non-uniform conditions on the outer surface of the casing.

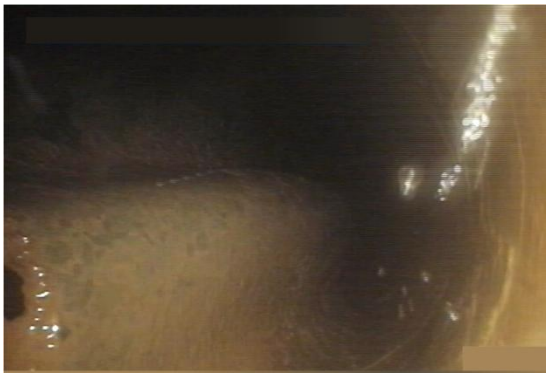

Figure 1: The buckling shape of a collapsed casing with external concrete support[1].

The collapse of casings in completed wells is the result of combined loads, e.g. pressure and temperature, and impurities in the casing and/or surrounding concrete.

It is well documented that geometric imperfections, e.g. average outside diameter, average wall thickness, eccentricity, and ovality, reduce the collapse resistance of casings. Defects, such as pitting due to external corrosion, external casing damage or other asymmetric conditions, also cause instability that can result in premature casing collapses.

Although the concrete should act as a pressure seal, concrete damage and impurities could lead to non-uniform conditions around the circumference of the casing. Instability can be caused by an off-center casing which can cause water/mud accumulation at the narrower side of the annulus due to lower flow rate during cementing. This could lead to fluid entrapment at one side of the annulus.

[1] Courtesy of HS Orka hf.

Material impurities and manufacturing residual stress result in decreased collapse resistance as well. Furthermore, corrosion can cause serious production casing failures. It can be very different between geothermal regions and even different within a geothermal region, for example from well to well or even varying with depth. For H_2S rich environments sulfide stress cracking (SSC) and hydrogen embrittlement can cause problems depending on the material selection for the steel casing (Kane 1996). No general solution of corrosion problems in geothermal wells exists and each case needs to be treated separately.

External to internal differential pressure is the main cause for the collapse of pipes. External casing pressure can be the result of thermally expanding fluids in the annulus during discharge. Wellbore pressure fluctuations due to cavitation and slug flow could also cause local casing collapse.

The maximum pumping pressure at the top of the well is described with

$$P_{pump} = P_{CR} - P(z)$$

where P_{CR} is the API rated collapse resistance of the casing, z is the casing depth and *P(z)* is the hydrostatic differential pressure of external concrete and internal water at the bottom of the casing. While the casing is being cemented on the outside, the inside is filled with cold water. If however this is neglected and in addition the external concrete pumping pressure gets too high, the casing can collapse due to excessive external pressure. Excessive pumping pressure could also merely create a deformation in the casing which could end in collapse due to subsequent wellbore loads, e.g. cyclic thermal loading.

Cracked or otherwise damaged concrete can also cause external pressure load on the casing, for example if small steam channels form or if water is present in the annulus when the well is discharged.

The effect of temperature is twofold since it produces thermal stresses in the casing and lowers the strength of the material. The latter occurs at high temperatures, around 300°C and above. Collapse of pipes as a result of temperature loading is not as well documented as collapse from external pressure, but cyclic temperature loading could ultimately lead to collapse or tearing of the casing.

A combination of geometric imperfections, material impurities and dynamic loading, such as local cavitation or rapid temperature change during discharge (or cooling), are likely causes of casing collapse.

MODELING

The finite element method (FEM) is used to construct a three dimensional model of the casing. The model is divided into two parts, thermal and structural. If thermal loads are to be included in the structural analysis, the change in temperature is first calculated in the thermal part of the model and the temperature distribution results are then used as load for the structural part. Eigenvalue buckling analysis is used to predict the theoretical collapse strength and the collapse mode shapes of the casing. The eigenvalue analysis is a linear solution method in which nonlinear properties, e.g. interaction of contacting surfaces, are not taken into account. Nonlinear buckling analysis is then used to account for nonlinearities which are found in the (i) material properties, (ii) large geometrical displacements and (iii) connectivity between contacting surfaces (contact elements). The limit load of the casing is obtained and stabilization is used to track the post-buckling shape of the casing.

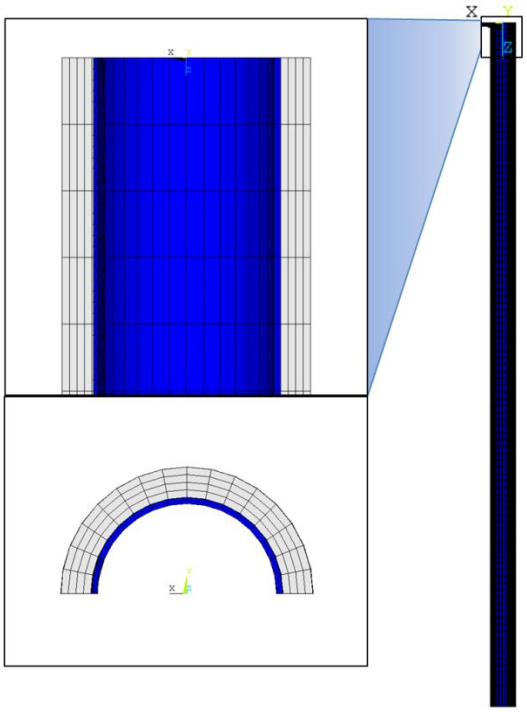

Figure 2: The geometry of the finite element model.

Available data on the stress-strain behavior of K55 casing steel and compressive strength of the concrete is used in the model. The stress-strain curves for the casing steel were obtained from standardized tensile tests (Karlsdottir 2009). The maximum compressive strength of concrete is defined as 27.6 MPa in the analysis. When the maximum compressive strength is reached the concrete is assumed to yield plastically. The material properties used in the FE analysis are listed in Table 1.

Table 1: Material properties used in the FE analysis (non-linear MP are discussed in the text).

	Steel	Concrete
Young's modulus (E) [GPa]	205	2,79
Poisson's ratio (γ)	0.3	0.15
Density (ρ) [kg/m^3]	7850	1666
Th.conductivity (K) [W/(m°C)]	46	0.81
Specific heat (c) [kJ/kg°C]	0.49	0.88
Thermal expansion (α) [1/°C]	12e-6	9e-6
Compressive strength (f_c) [MPa]	-	27.6
Coefficient of friction (μ)	0.5	
Max shear stress (τ_{max}) [MPa]	0.72	

The finite-element program Ansys is used to construct the model. Contact element pairs are used between contacting surfaces. Their main purpose is to prevent surfaces to intersect each other, while still allowing gap formation and tangential movement between casing and concrete. The Coulomb friction model is used to describe friction between contacting surfaces, where they can withstand shear stresses up to a certain magnitude across their interface before they start sliding relative to each other(Release 11.0 documentation for ANSYS 2007). Once the equivalent shear stress exceeds τ_{max} relative sliding begins. The friction model is defined as:

$$\tau_{lim} = \mu P + b$$
$$|\tau| \leq \tau_{lim}$$

where τ is the equivalent shear stress, τ_{lim} is the limit shear stress, μ is the isotropic coefficient of friction, b is the contact cohesion and P is the contact normal pressure, see Figure 3 for the graphical interpretation of the Coulomb friction model.

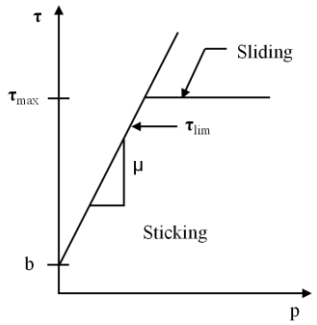

Figure 3: The Coulomb friction model in Ansys (Release 11.0 documentation for ANSYS 2007).

The geometry of the casing model is shown in Figure 2. A 12 meter section of the production casing is modeled in three dimensions. The concrete around the production casing is also included and for simplification external casings are not included. No radial displacement is allowed at the outer radial boundary of the concrete and axial displacements are constrained at both ends. The geometrical parameters that are used in the analysis are shown in Table 2. Half of the casing is modeled, which is possible due to the symmetry of the casing and its collapse shape. The thickness of the pipe wall is scaled with the manufacturing tolerance which is assumed to be −12,5% in the analysis.

Table 2: Geometrical parameters for the FE analysis.

	in	mm
Outer diameter of casing (*D*)	13 3/8	339.7
Thickness of casing (*t*)	0.48	12.2
Thickness of concrete (t_c)	2.10	53.4

Due to the perfect geometry of the model some imperfections or perturbations need to be introduced to create instability in the structure. Instead of applying a small radial force, which is a common practice, instability is created with randomly distributed material imperfections in the steel casing. These imperfections are included in the casing as small variations in material properties. Overview of the diminished casing used in the analysis can be seen in Table 3.

Table 3: Diminished casing overview

	%
Manufacturing tolerance	-12.5
Random material imperfections	20
Local external defect	10-50 of thickness

The effect of a small local defect, located on the outside of the production, casing is also analyzed. The size and shape of the defect is controlled by three parameters; thickness, angle size and length, see Figure 4. The defect can be interpreted as pit corrosion, defect or damage for example from scratching while running down the casing.

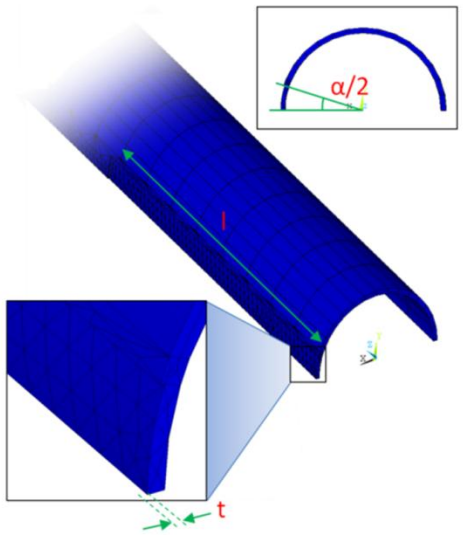

Figure 4: Size and shape of the external defect of the casing.

RESULTS

Eigenvalue buckling analysis is used to predict the theoretical collapse strength or the bifurcation point of a perfectly round casing subjected to uniform external pressure. Manufacturing tolerance of −12,5% is used to scale the wall thickness of the casing. Theoretical collapse strength values for mode shapes 1-8 are listed in Table 4 and the obtained collapse mode shapes can be seen in Figure 5.

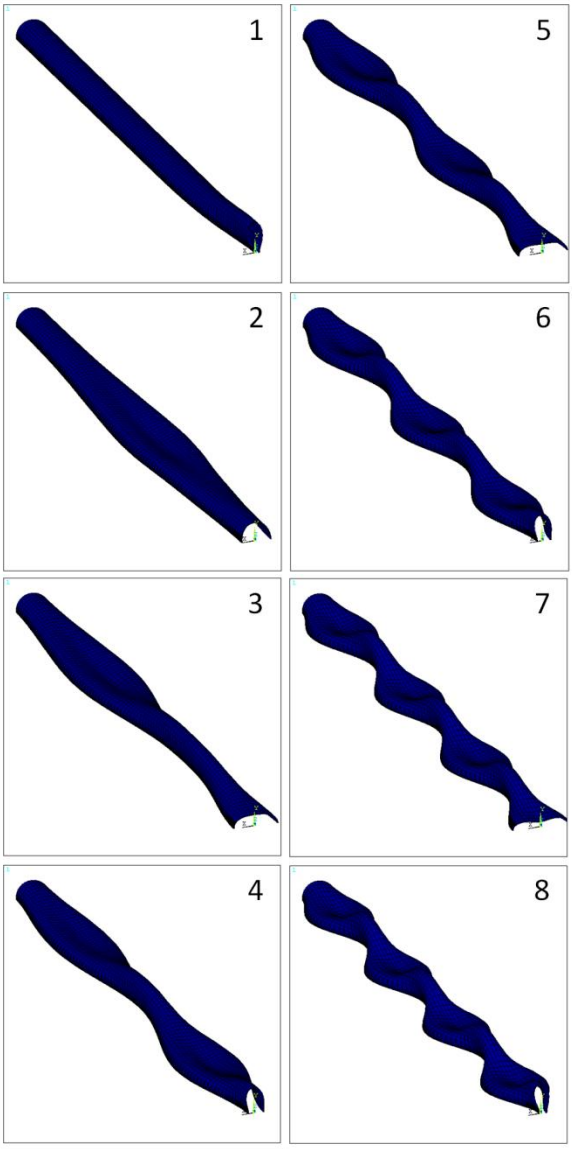

Figure 5: Collapse mode shapes 1-8 of the production casing (eigenvalue buckling analysis).

The theoretical collapse strength values obtained from the eigenvalue buckling analysis are slightly higher than the calculated API collapse resistance which is calculated as 13.4 MPa. There are no imperfections in the casing and the standard is known to provide rather conservative values for the collapse resistance. This implies that the eigenvalue buckling analysis underestimates the actual limit load of the casing although the results give a close match to the API collapse resistance.

Table 4: Theoretical collapse strength of the modeled casing using eigenvalue buckling analysis. API collapse resistance of this casing is calculated as 13.4 MPa.

Mode shape nr.	Theoretical collapse strength [MPa]	% of API collapse resistance
1	14.4	107.1
2	14.5	107.9
3	14.5	108.4
4	14.7	109.6
5	15.1	112.4
6	15.7	117.1
7	16.7	124.9
8	18.1	135.3

Nonlinear buckling analysis is used to predict the actual collapse limit load. Nonlinearities are now accounted for the casing. Additionally, the first mode shape from the eigenvalue buckling analysis is scaled down and used as perturbation to the initial geometry for the nonlinear buckling analysis. The limit load for the collapse is determined as 21.6 MPa, see Figure 6, which is higher than the theoretical collapse strength (bifurcation point) obtained in the eigenvalue buckling analysis. This is in agreement with the statement above that the linear eigenvalue buckling analysis probably underestimates the collapse strength of the casing.

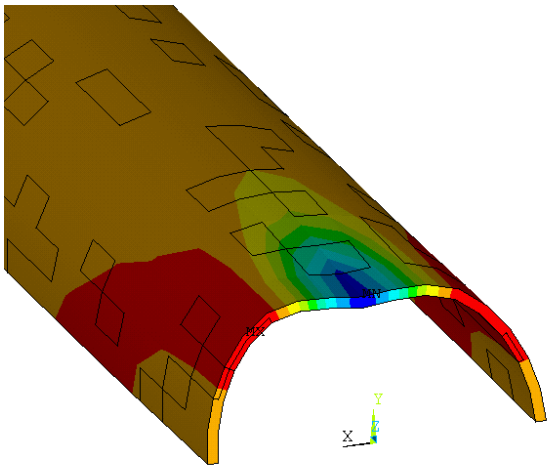

Figure 6: Initiation of collapse of a casing without geometrical defect. A nonlinear buckling analysis with the first mode shape scaled and used as perturbation. Collapse occurs at 21.6 MPa.

In Figure 7, load-displacement collapse curves are plotted for a perfectly round casing as well as a casing mode shape perturbation. The collapse limit load of a perfectly round casing is 38.4 MPa. For first mode shape perturbation the collapse occurs at 26.4 MPa and 21.6 MPa for scaling constants of 0.0005 and 0.001, respectively.

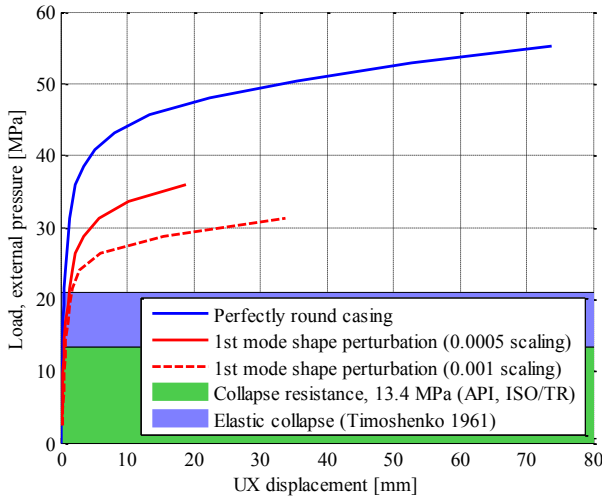

Figure 7: Effect of initial geometry on collapse. Perfectly round casing and mode shape perturbation. Results from a nonlinear buckling analysis.

The effect of ovality on collapse strength of the casing is analyzed. Ovality of pipes is defined as

$$\text{Ovality} = \frac{D_{max} - D_{min}}{D}$$

where D_{max} is the maximum outer diameter, D_{min} is the minimum outer diameter and D is the mean outer diameter.

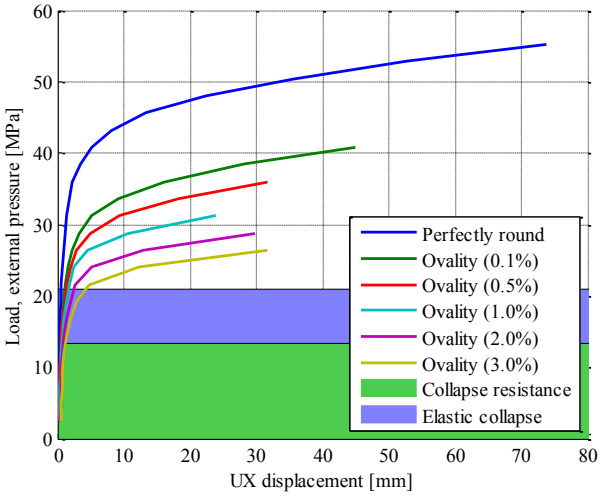

Figure 8: Effect of casing ovality on collapse. Results from a nonlinear buckling analysis.

Collapse curves of casings with ovality of 0.1% - 3.0% can be seen in Figure 8 and the collapse limit loads are listed in Table 5.

The effect of a geometric defect on the external surface of the casing is analyzed. First, the extreme case is analyzed where the defect depth is 0.5 times the casing thickness, 20° in circumference and one meter long. The collapse resistance of a casing with and without the structural support of the external concrete is analyzed as well, see Figure 9.

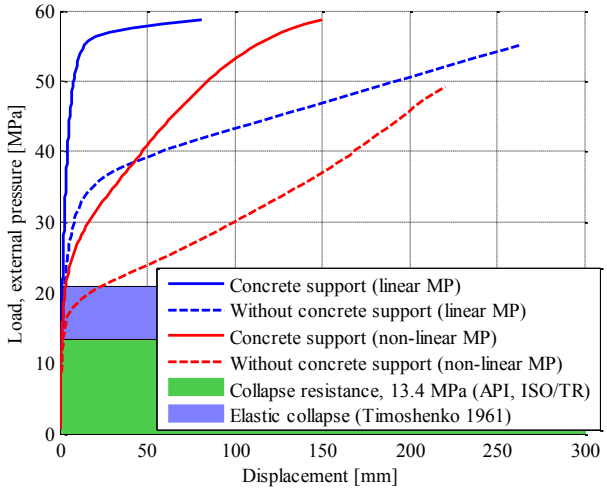

Figure 9: The effect of concrete structural support to the casing. Load-displacement collapse and post-collapse curves of an extreme defect case where the defect depth is 50% of the casing thickness.

The effect of nonlinear material properties, i.e. nonlinear stress-strain curves for K55 steel, are also compared and can be seen in Figure 9. The collapse limit load of the casing without concrete support is 14.4 MPa and with concrete support it increases to 18.1 MPa. Using linear material properties, the collapse limit load for same cases is 37.2 MPa and 56.4 MPa. When nonlinear material properties are used, plastic deformations take place which creates instability and leads to collapse. Conversely, when linear material properties are used, the casing remains stable until it collapses elastically. Why the elastic collapse does not match the theoretical elastic collapse, seen in blue box on the graphs, can be explained by the *D/t* ratio of the analyzed casing which collapse is determined by the transition between plastic and elastic collapse. The collapse and post-collapse shape with and without concrete structural support can be seen on the section diagrams in Figure 10.

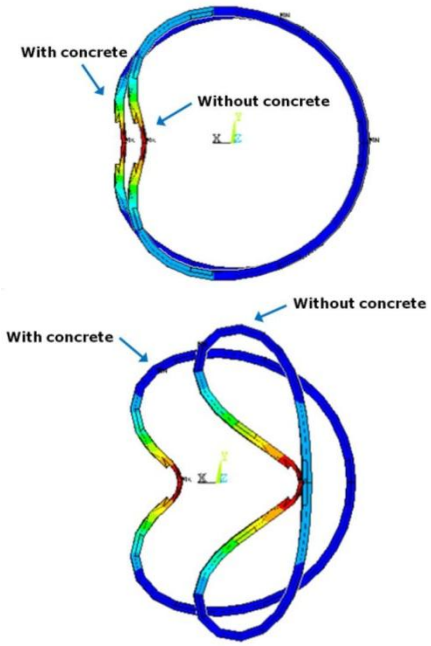

Figure 10: Collapse shapes of a casing with external defect depth of 50% the casing thickness, with and without concrete support (concrete not shown). Initiation of collapse (above) and post-collapse (below).

The effect of defect dept on the collapse shape of a casing supported by external concrete is analyzed as well. Defect depths of 10% to extreme 80% of the casing thickness can be seen in Figure 12. At 10% the defect merely makes the casing unstable but the location of the defect does not dominate the location of the collapse. At 20-30% the collapse is located at the defect but the deformation is relatively small.

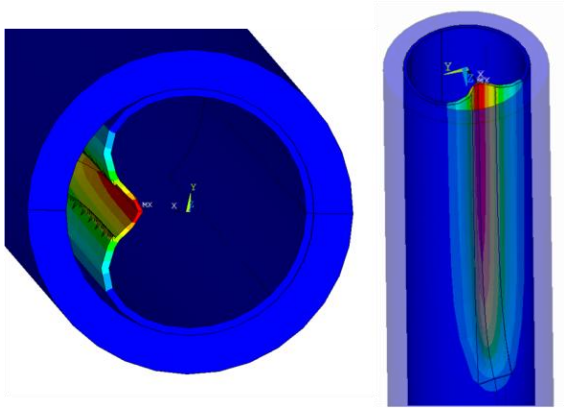

Figure 11: A collapsed casing with external defect depth of 40% of the thickness of the casing. Collapse load of 15.3 MPa.

At 40% defect depth, also seen in Figure 11, the deformation of the collapse becomes substantial, both inward and along the length. The radial displacement is 85mm and the length of the deformation is approximately 2 meters, twice as long as the defect length. For the cases of 50% to 60%, which are extreme cases unlikely to exist in reality, the deformation is similar to the 40% case, but cases above 70% the collapse becomes local to the defect and begins to resemble plate buckling. Collapse curves of various defect depths can be seen in Figure 13 and corresponding limit loads are listed in Table 5.

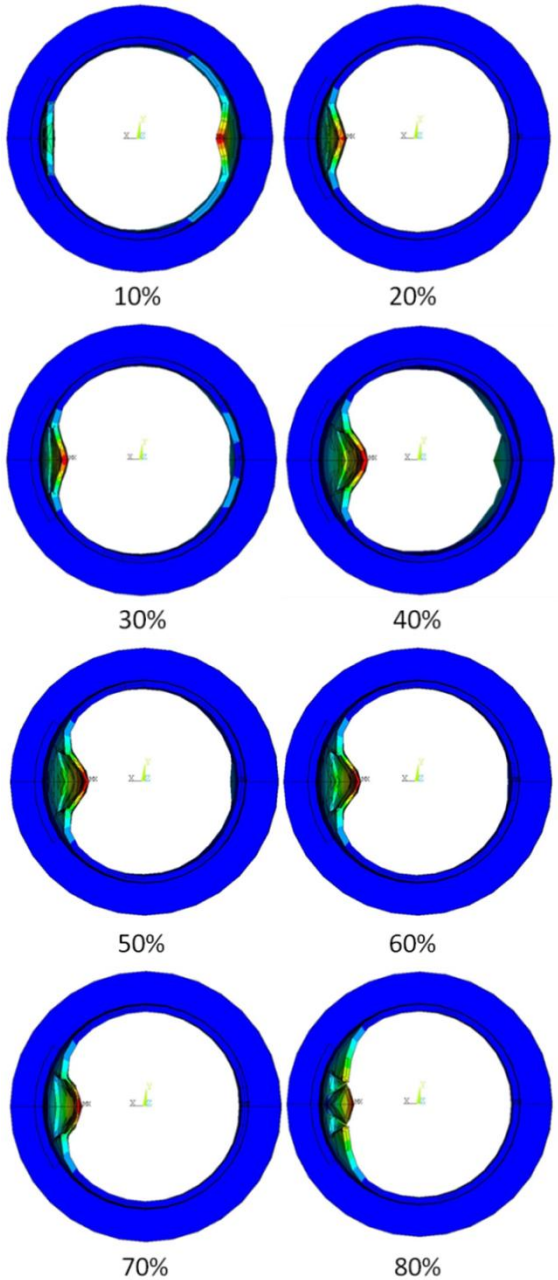

Figure 12: Effect of external defect depth on the collapse shape (percentage of casing thickness). End view of the casing and external concrete.

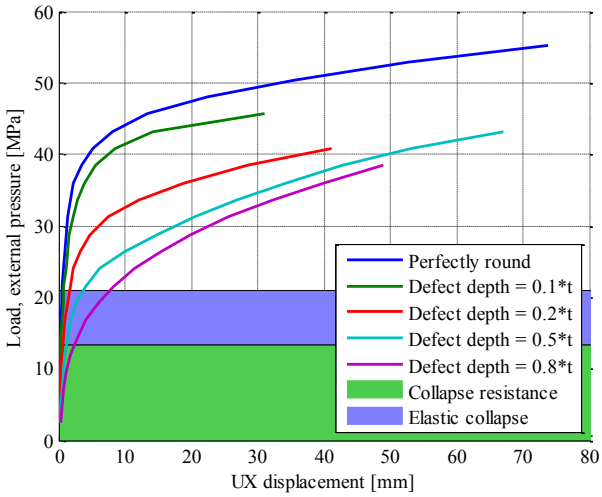

Figure 13: Effect of external defect depth on collapse.

A summary of the effect of initial geometry on collapse limit load can be seen in Table 5.

Table 5: Summary; effect of initial geometry on collapse. Mode shape perturbation, ovality and external defect. API collapse resistance of this casing is calculated as 13.4 MPa.

Initial geometry	Collapse limit load [MPa]	% of API collapse resistance
Without external concrete:		
Perfectly round	38.4	287
1st mode shape (0.0005)	26.4	197
1st mode shape (0.001)	21.6	161
Ovality (0.1%)	26.4	197
Ovality (0.5%)	24.0	179
Ovality (1.0%)	22.8	170
Ovality (2.0%)	21.0	157
Ovality (3.0%)	19.8	148
External defect (0.5*t)	14.4	107
With external concrete:		
External defect (0.1*t)	33.6	251
External defect (0.2*t)	25.2	188
External defect (0.5*t)	15.6	116
External defect (0.8*t)	12.0	89.6

The effect of a small deformation due to external pressure and its stimulus on subsequent collapse due to cyclic thermal loads is analyzed. A casing with external defect depth of 40% of the casing thickness is used in the analysis. The external pressure, which can be looked at as an excessive concrete pumping pressure, generates a small permanent deformation in the casing. Pressure is excluded from the analysis after the first load step to observe the thermal effect.

The thermal distribution for the cyclic thermal analysis can be seen in Figure 14.

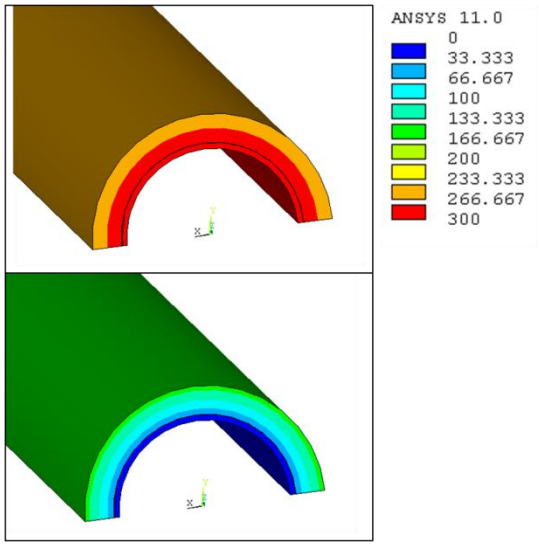

Figure 14: Thermal load used in the analysis; warm-up (above) and cooling (below).

The load history used in the analysis consists of external pressure which is then removed to see the resulting plastic deformation, following is cyclic thermal load which consists of a temperature difference of 300°C. This is a steady-state analysis so transient effects, such as rapid cooling, are not included. Pressure, reaching from 10 MPa to excessive 20 MPa, is subjected on the external surface of the casing which for pressure above 10 MPa results in plastic deformation.

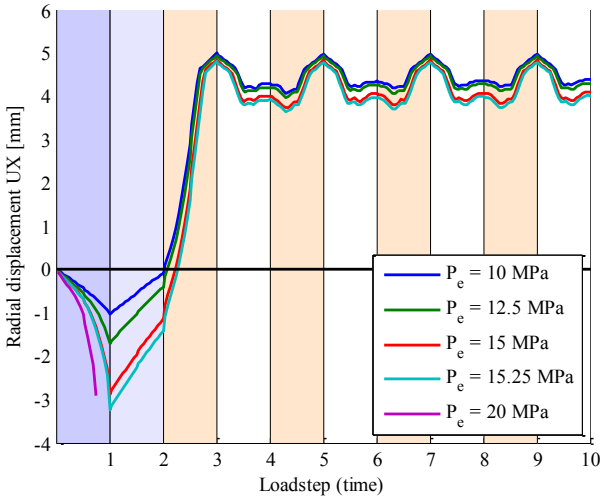

Figure 15: Initial external pressure and its effect on subsequent deformations. Blue: external pressure load, light blue: pressure removed, red: warm-up to 300°C, white: cooling.

Pressure above 15.3 MPa collapses the casing before temperature load is applied. Radial displacement curves can be seen in Figure 15. During cooling, stress relaxation is followed by tensile stress buildup in the casing, which goes beyond the proportional limit of the stress-strain curve of the steel. Because the radial displacement is still positive, this reverses the displacement of the defect, initially moving inward, forcing the displacement outwards again. By using linear material properties, see Figure 16, this does not occur. As the load history shows, subsequent collapse due to excessive initial pressure does not occur.

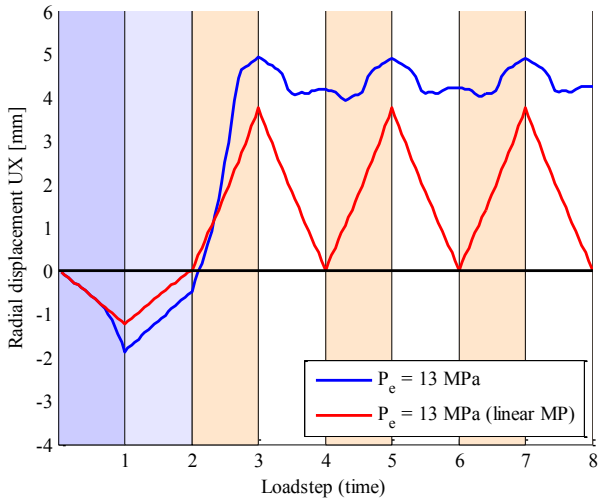

Figure 16: Nonlinear material properties and linear material properties compared.

CONCLUSION

In this study collapse limit loads of casings were analyzed with respect to pressure and temperature loads combined with casing imperfections with and without external concrete support. Eigenvalue buckling analysis was used to find the collapse mode shapes of a geometrically perfect casing. Nonlinear buckling analysis showed that the limit load for the casing was higher than the theoretical collapse strength (bifurcation point) of the eigenvalue buckling analysis, indicating that the eigenvalue buckling analysis underestimated the collapse strength of the casing.

The effect of initial geometry on collapse was analyzed. The collapse limit load of a perfectly round casing was compared to casings with geometry perturbation of the first mode shape from the eigenvalue buckling analysis. The casings with the mode shape perturbation showed reduced collapse strength of approximately 30-50%, using two scaling factors for the first mode shape. The reduction in collapse strength due to ovality was also analyzed. It showed that slight ovality reduces the collapse strength of the casing substantially. The effect of external defect and the defect depth on the collapse strength and collapse shape was analyzed. Modeled collapse shapes of a casing subjected to external pressure with and without the support of concrete were obtained. The latter resembled bulge collapse shapes documented in high temperature wells.

A load history was used consisting of external pressure followed by cyclic temperature difference of 300°C. The results showed that the initial pressure did not result in subsequent collapse. This is partly due to the nonlinear behavior of stress-strain curves of steel when reaching beyond the proportional limit.

It is apparent that a combination of factors cause casing failures. The load, consisting of temperature and pressure changes, and the load history is probably the main contributor. When subjected to load, imperfections in casings and surrounding concrete have also proved to play a big role in the generation of casing failures such as casing collapse.

Future work will involve analyzing more load histories and including transient loads, such as wellbore pressure fluctuations due to cavitation and slug flow, as well as further studying casing and concrete imperfections.

ACKNOWLEDGMENT

This work was supported by the University of Iceland research fund, the Technology Development Fund at RANNIS - The Icelandic Center for Research, the Innovation Center Iceland and GEORG - Geothermal Research Group. Their support is much appreciated.

REFERENCES

10400:2007(E), ISO/TR. *ISO/TR 10400, Petroleum and natural gas industries - equations and calculations for the properties of casing, tubing, drill pipe and line pipe used as casing or tubing.* Geneva: ISO copyright office, 2007.

Andrea P. Assanelli, Rita G. Toscano, Eduardo N. Dvorkin. „Analysis of the Collapse of Steel Tubes Under External Pressure.“ *Computational Mechanics*, 1998.

Björnsson, G., Ragnars, K., Sigfússon, S., Karlsson, Þ. *Styrkleiki fóðurröra í háhitaborholum (OS JHD 7805) (in Icelandic).* Reykjavík: Orkustofnun, 1978.

Bulson, P. S. „The Stability of Underground Cylindrical Shells.“ Í *Developments in Thin-Walled Structures - 1*, by J Rhodes og A. C. Walker, 53-80. Essex, England: Applied Science Publishers, 1983.

C. R. Kennedy, J. T. Venard. *Collapse of Tubes by External Pressure.* U. S. Atomic Energy Commision, 1962.

Chater, E., og J. W. Hutchinson. „On the Propagation of Bulges and Buckles.“ *Journal of Applied Mechanics*, 1984.

Fairbairn, William. „On the Resistance of Tubes to Collapse.“ *Philosophical Transactions of the Royal Society of London*, 1858: 389-413.

Kalil, Issa A., McSpadden, Albert R. „Casing Burst Stresses in Particulate-filled Annuli: Where's the Cement?“ *SPE/IADC Drilling Conference and Exhibition, 1-3 March 2011*. Amsterdam, The Netherlands: 2011. SPE/IADC Drilling Conference and Exhibition, 2011.

Karlsdottir, S. N., Thorbjornsson, I. O. „High Temperature Geothermal Wells – Center of Excellence in Iceland - Phase I: Corrosion testing of steel in high temperature geothermal wells in Iceland.“ Technical Report for RANNIS (The Icelandic Centre for Research), Reykjavik, Oct., 2009.

Magneschi, P., Bagnoli, C. , Lazzarotto, A. , Ricciardulli, R. „Structural Models for the Analysis of Stresses in the Casings of Geothermal Wells.“ World Geothermal Congress, 1995.

Naoto Sakakibara, Stelios Kyriakides, Edmundo Corona. „Collapse of Partially Corroded or Worn Pipe Under External Pressure.“ *International Journal of Mechanical Sciences*, 2008: 1586-1597.

Netto, T.A. „On the effect of narrow and long corrosion defects on the collapse pressure of pipelines.“ *Applied Ocean Research*, 2009: 75-80.

Release 11.0 documentation for ANSYS. SAS IP, Inc., 2007.

Southon, J. N. A. „Geothermal Well Design, Construction and Failures.“ Auckland, New Zealand: Proceedings World Geothermal Congress 2005, 2005.

Thorhallsson, Sverrir. „New Developments in Geothermal Drilling.“ *Workshop for Decision Makers on Geothermal Projects in Central America*. El Salvador: UNU-GTP and LaGeo, 2006.

Timoshenko, S. P., og Gere J. M. *Theory of Elastic Stability.* New York: McGraw-Hill, 1961.

Watkins, Reynold King, and Loren Runar Anderson. *Structural mechanics of buried pipes.* CRC Press LLC, 2000.